

Version 1.0  
(Do Not Cite or Quote Without Permission)

# **AUTISM AND EEG PHASE RESET: A UNIFIED THEORY OF DEFICIENT GABA MEDIATED INHIBITION IN THALAMO- CORTICAL CONNECTIONS**

Thatcher, R. W. <sup>1</sup>, North, D. M. <sup>1</sup>, Neubrandner, J. <sup>2</sup>, Biver, C. J. <sup>1</sup>, Cutler, S. <sup>2</sup>, and  
DeFina, P. <sup>3</sup>

EEG and NeuroImaging Laboratory, Applied Neuroscience Research Institute., St.  
Petersburg, FL<sup>1</sup>, the Comprehensive Neuroscience Center , Menlo Park, NJ<sup>2</sup> and the  
International Brain Research Foundation, Menlo Park, N.J.<sup>3</sup>

**Send Reprint Requests To:**  
**Robert W. Thatcher, Ph.D.**  
**NeuroImaging Laboratory**  
**Applied Neuroscience Res. Inst.**  
**St. Petersburg, Florida 33722**  
**(727) 244-0240, rwthatcher@yahoo.com**

## ABSTRACT

**Objectives:** The purpose of this study was to explore the relationship between EEG phase reset in autistic spectrum disorder (ASD) subjects as compared to age matched normal subjects.

**Methods:** The electroencephalogram (EEG) was recorded from 19 scalp locations from 54 autistic subjects and 241 normal subjects ranging in age from 2.6 years to 11 years. Complex demodulation was used to compute instantaneous phase differences between all pairs of electrodes and the 1<sup>st</sup> & 2nd derivatives were used to measure phase reset by phase shift duration and phase lock duration.

**Results:** In both short (6 cm) and long (21 – 24 cm) inter-electrode distances phase shift duration in ASD subjects was significantly shorter in all frequency bands but especially in the alpha-1 frequency band (8 – 10 Hz) ( $P < .0001$ ). Phase lock duration was significantly longer in the alpha-2 frequency band (10 – 12 Hz) in ASD subjects ( $P < .0001$ ). An anatomical gradient was present with the occipital-parietal regions the most significant.

**Conclusions:** The findings in this study support the hypothesis that neural resource recruitment occurs in the lower frequency bands and especially the alpha-1 frequency band while neural resource allocation occurs in the alpha-2 frequency band. The results are consistent with a general GABA inhibitory neurotransmitter deficiency resulting in reduced number and/or strength of thalamo-cortical connections in autistic subjects.

Key Words: Autism, EEG phase reset, phase locking, phase shifting

## 1.0- Introduction

Autistic spectrum disorder (ASD) has been defined as a severe developmental brain disorder characterized by restricted and repetitive behavior, excessive attention to detail and reduced social and global integration including deficits in executive function, language and social interactions (Rapin and Dunn, 2003; Belmonte et al., 2004; Hill, 2004). The environmental and genetic sources of ASD are not known although there have been recent advances in the understanding of the nature of the neurophysiological deficits that are correlated with autism. Theories of reduced connectivity are prevalent and supported by magnetic resonance spectroscopy (MRS) that show reduced synapses in thalamic, basal ganglia, amygdala, hippocampus and cortical locations (Minshew and Petigrew, 1995; Minshew and Williams, 2007; Hardan et al, 2008; Perich-Alsina et al, 2002; Page et al, 2006; Kleinhans et al, 2007; Otsuka et al, 1999). Disorders of sensory gating in evoked potential studies (Orekhova et al, 2008) and disorders of connectivity in fMRI (Kana et al, 2007) and disorders of coherence in electroencephalogram (EEG) studies (Cantor et al, 1987; Murias et al, 2007; Welsh et al, 2005; Vandenbroucke et al, 2008, Brock et al, 2002 and Orekhova et al, 2008) suggest a common neurophysiological basis for ASD, namely a general neural synchronization disorder.

EEG studies of autism typically show a 'U' shaped function of power versus frequency with elevated power at low and high frequencies and reduced power in the alpha frequency band (Cantor et al, 1987; Murias et al, 2007). Murias et al (2007) using 122 channel high density EEG showed elevated power in the theta (3 – 6 Hz) and the beta frequency band (13 – 17 Hz) with reduced power in the alpha frequency range (9 – 10 Hz). Cantor et al (1987) also reported elevated power in the lower and higher frequency bands as well as reduced power in the alpha band in autistic subjects. Orekhova et al (2007, 2008) reported excess power in the gamma frequency range which was also correlated with lower suppression of the P50 sensory gating response and less inhibition in autistic subjects. Elevated coherence in autistic subjects was reported for all frequency bands in Cantor et al (1987) while Murias et al (2007) reported elevated coherence in the delta, theta and beta frequency bands but not in the alpha-1 (8-10 Hz) frequency band. Excess high frequency EEG measures have indicated an imbalance in GABA inhibitory neurons (Brown et al, 2005; Orekhova et al, 2008). These EEG studies are also consistent with reduced synchronization in autistic subjects (Kana et al, 2008; Welsh et al, 2005) and with models of synaptic disconnection and lower levels of differentiation in autistic subjects (Brock et al, 2002; Rippon et al, 2007).

Deficient GABA neurotransmitters have recently been suggested as a unifying cause of ASD (DeLong, 2007; Kana et al, 2007; Orekhova et al, 2008). This is an important unifying hypothesis because GABA is the only inhibitory neurotransmitter in the human brain and GABA is the primary neurotransmitter responsible for the rapid synchronization of populations of neurons as well as rhythmic discharges in thalamo-cortical circuits responsible for the genesis of all EEG rhythms (Steriade et al, 1990; Buzsaki, 2006). The rise and fall times and duration of the bursting of inhibitory neurons determines the timing and gating in the thalamic relay nuclei and the time and sequencing in the hippocampus and cortex all of which are mediated by GABA receptors (Mainen and Sejnowski, 1995; 1996; Thomson, 2000a; 2000b; Buzsaki, 2006). There are two chemically different categories of the GABA inhibitory neurotransmitter receptors with: 1- GABA<sub>A</sub> & C composed of ionotropic subunits with GABA-A responsible for fast neural responses and rapid rise and fall times of inhibitory post synaptic potentials (IPSPs) and the production of hi-beta and gamma EEG frequencies > 20 Hz (Kuffler and Edwards, 1958; Buzsaki, 2006; Steriade, 2005) and, 2- GABA<sub>B</sub> composed of a metabotropic 'G' protein is responsible for long duration IPSPs and EEG rhythms in the mid range of 5 to 18 Hz (low theta to low beta EEG frequencies) (Bowery, 2002; Steriade, 2005). Both types of GABA receptors are present in

the thalamus and other brain regions, however as hypothesized in the present study, the link to EEG and autism is best understood by thalamo-cortical mechanisms of synchronization mediated by GABA<sub>B</sub> involved in the mid range frequencies (Colomb et al, 2006; Miller, 1996; Steriade, 2005) and GABA-A involved in hi-beta and gamma frequencies (Bright et al, 2007; Okada et al, 2000). The EEG findings of a 'U' shaped power spectrum in autistic subjects (Cantor et al, 1987; Murias et al, 2007) with elevated slow and high frequencies and reduced power and deviant coherence measures is consistent with an hypothesis of deficient GABA mediated thalamo-cortical circuits in ASD subjects.

Whether deficiencies in thalamo-cortical GABA (A) or (B) or both are involved in autism or the extent of distorted synchrony is not easy to measure or resolve using standard EEG measures such as coherence. This is because coherence is a general estimate of the consistency of phase differences in a particular frequency band but with little or no time resolution and coherence is susceptible to volume conduction. Recently measures of phase reset that involve phase locking and phase shift have been shown to underlay the mechanisms of coherence and provide for high temporal resolution and minimal volume conduction distortion (Freeman et al, 2003; 2006). Phase reset is a useful measure of the rapid creation and destruction of multistable spatial-temporal patterns in evoked response and spontaneous EEG studies (Breakspear and Terry, 2002a, 2002b; Rudrauf et al, 2006; Le Van Quyen, 2003). The patterns of spontaneously occurring synchronous activity involve the temporary creation of differentiated and coherent neural assemblies at local and large scales (Breakspear and Terry, 2002a; 2002b; Rudrauf et al, 2006; Stam and de Bruin, 2004; Varela, 1995; Freeman and Rogers, 2002). The dynamic balance between synchronization and desynchronization is considered essential for normal brain function and abnormal balance is often associated with pathological conditions such as epilepsy (Lopes da Silva and Pihl, 1995; LeVan Quyen et al, 2001a; 2001b; Chevez et al, 2003; Netoff and Schiff, 2002), schizophrenia (Lere et al., 2002) and dementia (Stam et al., 2002a; 2002b).

Studies by Freeman and Rogers (2002) and Freeman et al (2003) show that the spontaneous EEG is made up of a mixture of synchronous processes that involve rapid phase shifts (approx. 30 msec to 80 msec) followed by a longer duration of phase locking (e.g., 100 msec to 800 msec) of clusters and sub-clusters of neurons that are followed by another phase shift and subsequent phase locking of different clusters of neurons. The integrated rapid sequencing of phase shifts followed by phase locking (i.e., the two fundamental components of phase reset) have been correlated to the alpha frequency band during cognitive tasks (Kahana; 2006; Kirschfeld, 2005; Tesche and Karhu, 2000), working memory (John, 1968; Rizzuto et al, 2003; Damasio, 1989; Tallon-Baudry et al, 2001), sensory-motor interactions (Vaadia et al, 1995; Roelfsema et al, 1997), hippocampal long-term potentiation (McCartney et al, 2004), consciousness (Cosmelli et al, 2004; Varela et al, 2001; John, 2002; 2005) and intelligence (Thatcher et al, 2008b). A recent study from this laboratory observed direct correlations between phase shift duration and intelligence as well as an inverse relationship between phase locking and intelligence (Thatcher et al, 2008b). The explanation of this correlation is that phase shift represents a process that identifies and recruits available neural resources, e.g, neurons not refractory or committed to other loops and that phase locking represents a binding together of synchronous neurons in interconnected loops that mediate momentary functions. The phase locked neurons are released by a subsequent phase shift and a different cluster of neurons is then phase locked and this process repeats in spatially distributed systems in the ongoing and dynamic EEG. Further, the time differences of phase shift between 6 cm vs 24 cm inter-electrode distances range from 5 msec to 15 msec which means that cortico-cortical conduction velocities can not explain these time differences. On the other hand, the thalamus that is only approximately 2 cm in the anterior-posterior plane can easily account for small time differences recorded at the scalp surface and the thalamus is a structure that is directly involved in cortical synchrony and dynamic sensory-motor gating (Steriade, 2005). In addition, GABA(A) & (B)

receptors are located in the thalamus and as reviewed previously are well positioned to orchestrate the timing of local and distant cortical phase shift and phase lock.

The purpose of the present study is to analyze differences between age matched normal subjects and ASD subjects with respect to phase shift duration and phase lock duration in order to evaluate the fine temporal detail of thalamo-cortical synchronization in autistic subjects. Differences in phase shift and lock durations in short vs long inter-electrode distances as well as differences between left and right hemispheres will be evaluated.

## **2.0 – Methods**

### **2.1 Subjects**

A total of 54 patients diagnosed with autism spectrum disorder (ASD) ranging in age from 2.6 to 10.74 years (mean = 7.25 yrs, st. dev. = 2.33 yrs; males = 47) were included in this study. The ASD patients were admitted to the Comprehensive Neuroscience Center and medically diagnosed as autistic spectrum disorder (ASD) based on DSM-IV criteria as well as various diagnostic instruments including, but not limited to the Childhood Autism Scale, Gilliam Autism Rating Scale-2, Autism Diagnostic Interview-R. A total of 241 age matched normal subjects (2.2 to 11 years; mean = 7.24 yrs, st. dev. = 2.3; males = 142) were recruited using newspaper advertisements in rural and urban Maryland (Thatcher et al, 1987; 2003; 2007). The inclusion/exclusion criteria were no history of neurological disorders such as epilepsy, head injuries and reported normal development and successful school performance. All of the school aged normal control children were performing at grade level in reading, spelling and arithmetic as measured by the Wide Range Achievement Test (WRAT) and none were classified as learning disabled nor were any of the school aged children in special education classes (Thatcher et al, 1987; 2003).

### **2.2 EEG Recording**

Power spectral analyses were performed on 58 seconds to 4 minutes and 25 second segments of EEG recorded during resting eyes open condition. The EEG was recorded from 19 scalp locations based on the International 10/20 system of electrode placement, using linked ears as a reference. The average reference and a Laplacian reference were not used because these reference methods involve mixing the amplitude and phase from different scalp locations resulting in phase and coherence distortions as shown by Rappelsberger (1989), Kamiński and Blinowska (1991) and Essl and Rappelsberger (1998). Eye movement electrodes were applied to monitor artifact and all EEG records were visually inspected and manually edited to remove any visible artifact. Each EEG record was plotted and visually examined and split-half reliability and test re-test reliability measures of the artifacted data were computed using the Neuroguide software program (NeuroGuide, v2.5.2). Split-half reliability tests were conducted on the edited EEG segments and only records with > 90% reliability were entered into the spectral analyses. The amplifier bandwidths were nominally 1.0 to 30 Hz, the outputs being 3 db down at these frequencies. The EEG was digitized at 128 Hz and then spectral analyzed using complex demodulation (Granger and Hatanaka, 1964; Otnes and Enochson, 1978). Phase shift duration and phase lock duration were computed from all possible electrode combinations of 171. The analyses involved computing mean phase shift and phase lock duration from intrahemispheric short inter-electrode distances of approximately 6 cm based on the International 10/20 system (O1/2-P3/4; O1/2-T5/6; P3/4-C3/4; C3/4-F3/4, F3/4-Fp1/2; Fp1/2-F7/8; F7/8-T3/4; Fp1/2-Fz; F3/4-Fz; C3/4-Cz; C3/4-Pz; P3/4-Pz and O1/2-Pz) and from long inter-electrode distances approximately 21cm – 24 cm based on the International 10/20

system (Fp1/2-T5/6; Fp1/2-P3/4; F7/8-T5/6; P3/4-F7/8; O1/2-F7/8; F3/4-T5/6; F3/4-P3/4; F3/4-O1/2; Fp1/2-Pz; F7/8-Pz; F3/4-Pz; T5/6-Fz; P3/4-Fz and O1/2-Fz).

EEG phase shift and phase lock durations were computed in the delta (1 – 4 Hz); theta (4 – 8 Hz); alpha1 (8 – 10 Hz); alpha2 (10 – 13 Hz); beta1 (13 – 15 Hz); beta2 (15 – 18 Hz) and hi-beta (25 – 30 Hz) frequency bands. Factors used in the multivariate analysis of variance were: 1- Hemisphere, 2- Direction, 3- Frequency band and 4- Inter-electrode distance with autism vs normal as the dependent variables.

### 2.3 – Complex Demodulation and Joint-Time-Frequency-Analysis

Complex demodulation was used in a joint-time-frequency-analysis (JTFA) to compute instantaneous coherence and phase-differences (Granger and Hatanaka, 1964; Otnes and Enochson, 1978; Bloomfield, 2000). This method is an analytic linear shift-invariant transform that first multiplies a time series by the complex function of a sine and cosine at the center frequency of each frequency band followed by a low pass filter (6<sup>th</sup> order low-pass Butterworth) which removes all but very low frequencies (shifts frequency to 0) and transforms the time series into instantaneous amplitude and phase and an “instantaneous” spectrum (Bloomfield, 2000). We place quotations around the term “instantaneous” to emphasize that, as with the Hilbert transform, there is always a trade-off between time resolution and frequency resolution. The broader the band width the higher the time resolution but the lower the frequency resolution and vice versa. Mathematically, complex demodulation is defined as an analytic transform (Z transform) that involves the multiplication of a discrete time series  $\{x_t, t = 1, \dots, n\}$  by sine  $\omega_0 t$  and  $\cos \omega_0 t$  giving

$$x'_t = x_t \sin \omega_0 t \quad (1)$$

and

$$x''_t = x_t \cos \omega_0 t \quad (2)$$

and then apply a low pass filter  $F$  to produce the instantaneous time series,  $Z'_t$  and  $Z''_t$  where the sine and cosine time series are defined as:

$$Z'_t = F(x_t \sin \omega_0 t) \quad (3)$$

$$Z''_t = F(x_t \cos \omega_0 t) \quad (4)$$

and

$$2[(Z'_t)^2 + (Z''_t)^2]^{1/2} \quad (5)$$

is an estimate of the instantaneous amplitude of the frequency  $\omega_0$  at time  $t$  and

$$\tan^{-1} \frac{Z'_t}{Z''_t} \quad (6)$$

is an estimate of the instantaneous phase at time  $t$ .

The instantaneous cross-spectrum is computed when there are two time series  $\{y_t, t = 1, \dots, n\}$  and  $\{y'_t, t = 1, \dots, n\}$  and if  $F[\ ]$  is a filter passing only frequencies near zero, then, as above  $R_t^2 = F[y_t \sin \omega_0 t]^2 + F[y_t \cos \omega_0 t]^2 = |F[y_t e^{i\omega_0 t}]|^2$  is the estimate of the amplitude of frequency  $\omega_0$  at time  $t$  and  $\varphi_t = \tan^{-1} \left( \frac{F[y_t \sin \omega_0 t]}{F[y_t \cos \omega_0 t]} \right)$  is an estimate of the phase of frequency  $\omega_0$  at time  $t$  and

$$F[y_t e^{i\omega_0 t}] = R_t e^{i\varphi_t}, \quad (7)$$

and likewise,

$$F[y'_t e^{i\omega_0 t}] = R'_t e^{i\varphi'_t} \quad (8)$$

The instantaneous cross-spectrum is

$$V_t = F[y_t e^{i\omega_0 t}] F[y'_t e^{-i\omega_0 t}] = R_t R'_t e^{i[\varphi_t - \varphi'_t]} \quad (9)$$

and the instantaneous coherence is

$$\frac{|V_t|}{R_t^2 R'^2} \equiv 1 \quad (10)$$

The instantaneous phase-difference is  $\varphi_t - \varphi'_t$ . That is, the instantaneous phase difference is computed by estimating the instantaneous phase for each time series separately and then taking the difference. Instantaneous phase difference is also the arctangent of the imaginary part of  $V_t$  divided by the real part (or the instantaneous quadspectrum divided by the instantaneous cospectrum) at each time point. We used the phase “straightening” method of Otnes and Enochson (1978) to remove the phase angle discontinuity, i.e., where 0 and 360 are at opposite ends while in the circular distribution  $0^0 = 360^0$ .

#### 2.4- Computation of the 1<sup>st</sup> and 2<sup>nd</sup> Derivatives of the Time Series of Phase Differences

The first derivative of the time series of phase-differences between all pair wise combinations of two channels was computed in order to detect advancements and reductions of phase-differences. The Savitzky-Golay procedure was used to compute the first derivatives of the time series of instantaneous phase differences using a window length of 3 time points and the polynomial degree of 2 (Savitzky-Golay, 1964; Press et al, 1994). The units of the 1<sup>st</sup> derivative are in degrees/point and represented in degrees per centisecond (i.e., degrees/cs = degrees/100 msec). The second derivative was computed using a window length of 5 time points and a

polynomial degree of 3 and the units are degrees per centiseconds squared (i.e., degrees/cs<sup>2</sup> = degrees/100 msec.<sup>2</sup>).

## 2.5 – Calculation of Phase Reset

The time series of 1<sup>st</sup> derivatives of the phase difference from any pair of electrodes was first rectified to the absolute value of the 1<sup>st</sup> derivative (see fig. 2). The sign or direction of a phase shift is arbitrary since two oscillating events may “spontaneously” adjust phase with no starting point (Pikovsky et al, 2003; Tass, 2007). The onset of a phase shift was defined as a significant absolute first derivative of the time series of phase differences between two channels, i.e.,  $d(\varphi_i - \varphi'_i)/dt > 0$ , criterion bounds =  $5^0$ . Phase stability or phase locking is defined as that period of time after a phase shift where there is a stable near zero first derivative of the instantaneous phase differences or  $d(\varphi_i - \varphi'_i)/dt \approx 0$ . The criteria for a significant 1<sup>st</sup> derivative is important and in the present study a threshold criteria of  $5^0$  was selected because it was  $> 3$  standard deviations where the mean phase shift ranged from 25 deg/cs to 45 deg/cs. Changing the threshold to higher values was not significant, however, eliminating the threshold resulted in greater “noise” and therefore the criteria of  $5^0$  is an adequate criteria. As pointed out by Blackspear and Williams (2004) visual inspection of the data is the best method for selecting an arbitrary threshold value and the threshold value itself is less important than keeping the threshold constant for all subjects and all conditions. Figure one illustrates the concept of phase reset. Phase differences over time on the unit circle are measured by the length of the unit vector  $r$ . Coherence is a measure of phase consistency or phase clustering on the unit circle as measured by the length of the unit vector  $r$ . The illustration in figure 1 shows that the resultant vector  $r_1 = r_2$  and therefore coherence when averaged over time  $\approx 1.0$  even though there is a brief phase shift. As the number of phase shifts per unit time increases then coherence declines because coherence is directly related to the average amount of phase locking or phase synchrony (Bendat and Piersol, 1980).

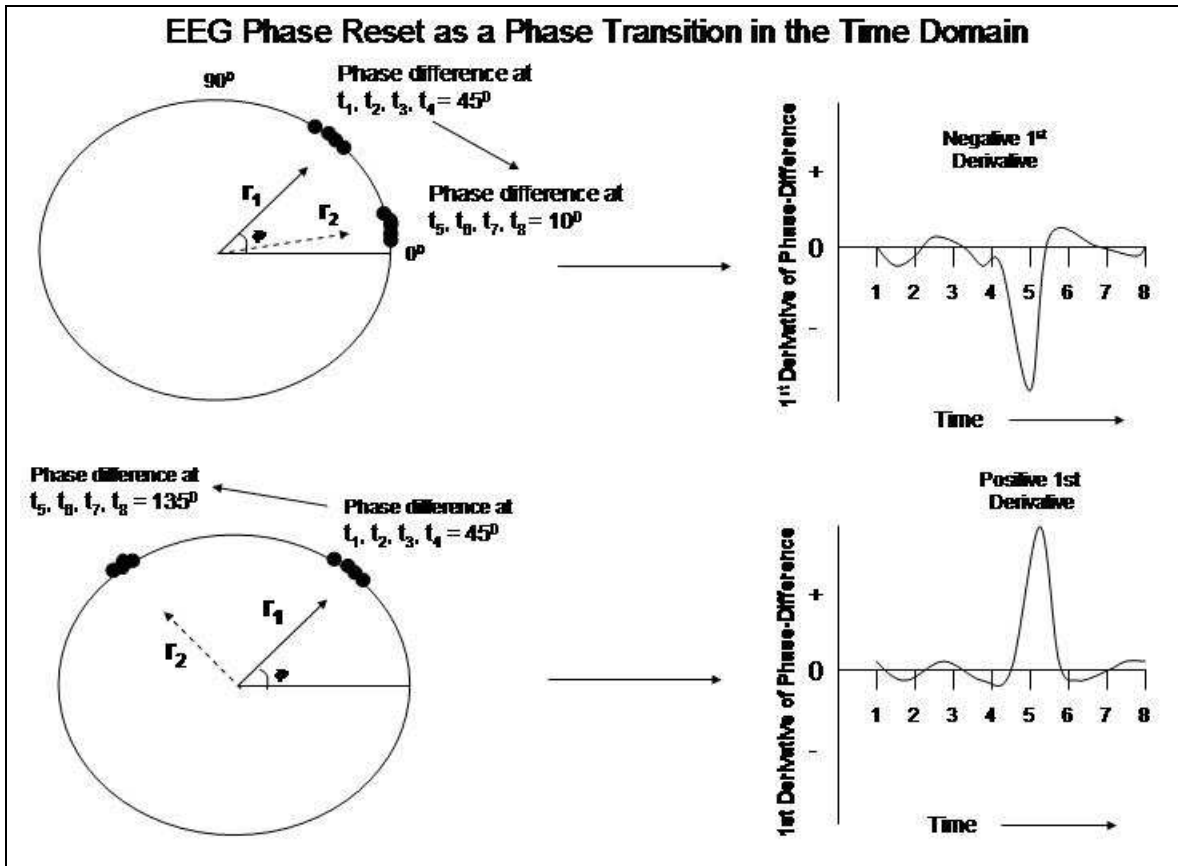


Fig. 1 – Illustrations of phase reset. Left is the unit circle in which there is a clustering of phase angles and thus high coherence as measured by the length of the unit vector  $r$ . The top row is an example of phase reduction and the top right is a time series of the approximated 1<sup>st</sup> derivative of the instantaneous phase differences for the time series  $t_1, t_2, t_3, t_4$  at mean phase angle =  $45^\circ$  and  $t_5, t_6, t_7, t_8$  at mean phase angle =  $10^\circ$ . The vector  $r_1 = 45^\circ$  occurs first in time and the vector  $r_2 = 10^\circ$  and  $135^\circ$  (see bottom left) occurs later in time. Phase reset is defined by a sudden change in phase difference followed by a period of phase locking. The onset of Phase Reset is between time point 4 and 5 where the 1<sup>st</sup> derivative is a maximum. The 1<sup>st</sup> derivative near zero is when there is phase locking and little change in phase difference over time. The bottom row is an example of phase advancement and the bottom right is the 1<sup>st</sup> derivative time series. The sign or direction of phase reset in a pair of EEG electrodes is arbitrary since there is no absolute “starting point” and phase shifts are often “spontaneous” and not driven by external events, i.e., self-organizing criticality. When the absolute 1<sup>st</sup> derivative  $\approx 0$  then two oscillating events are in phase locking and represent a stable state independent of the direction of phase shift (adapted from Thatcher et al, 2008a).

Figure 2 shows the time markers and definitions used in this study. As mentioned above the peak of the absolute 1<sup>st</sup> derivative was used in the detection of the onset and offset of a phase shift and the second derivative was used to detect the inflection point which defines the full-width-half-maximum (FWHM) and phase shift duration. As seen in Figure 2, Phase Reset (PR) is composed of two events: 1- a phase shift of a finite duration (SD) and 2, followed by an extended period of phase locking as measured by the phase lock duration (LD) and  $PR = SD +$

LD. Phase Shift duration (SD) is the interval of time from the onset of phase shift to the termination of phase shift where the termination is defined by two conditions: 1- a peak in the 1<sup>st</sup> derivative (i.e., 1<sup>st</sup> derivative changes sign from positive to zero to negative) and, 2- a peak in the 2<sup>nd</sup> derivative or inflection on the declining side of the time series of first derivatives. The peak of the 2<sup>nd</sup> derivative marked the end of the phase shift period. Phase shift duration is the difference in time between phase shift onset and phase shift offset or  $SD(t) = S(t)_{\text{onset}} - S(t)_{\text{offset}}$ . Phase lock duration (LD) was defined as the interval of time between the end of a significant phase shift (i.e., peak of the 2<sup>nd</sup> derivative) and the beginning of a subsequent significant phase shift, i.e., marked by the peak of the 2<sup>nd</sup> derivative and the presence of a peak in the 1<sup>st</sup> derivative or  $SI(t) = S(t)_{\text{offset}} - S(t)_{\text{onset}}$ . In summary, two measures of phase dynamics were computed: 1- Phase shift duration (msec) (SD) and, 2- Phase lock duration (msec) (LD). Figure two illustrates the phase reset metrics and figure three shows an example of the computation of phase reset metrics in a single subject.

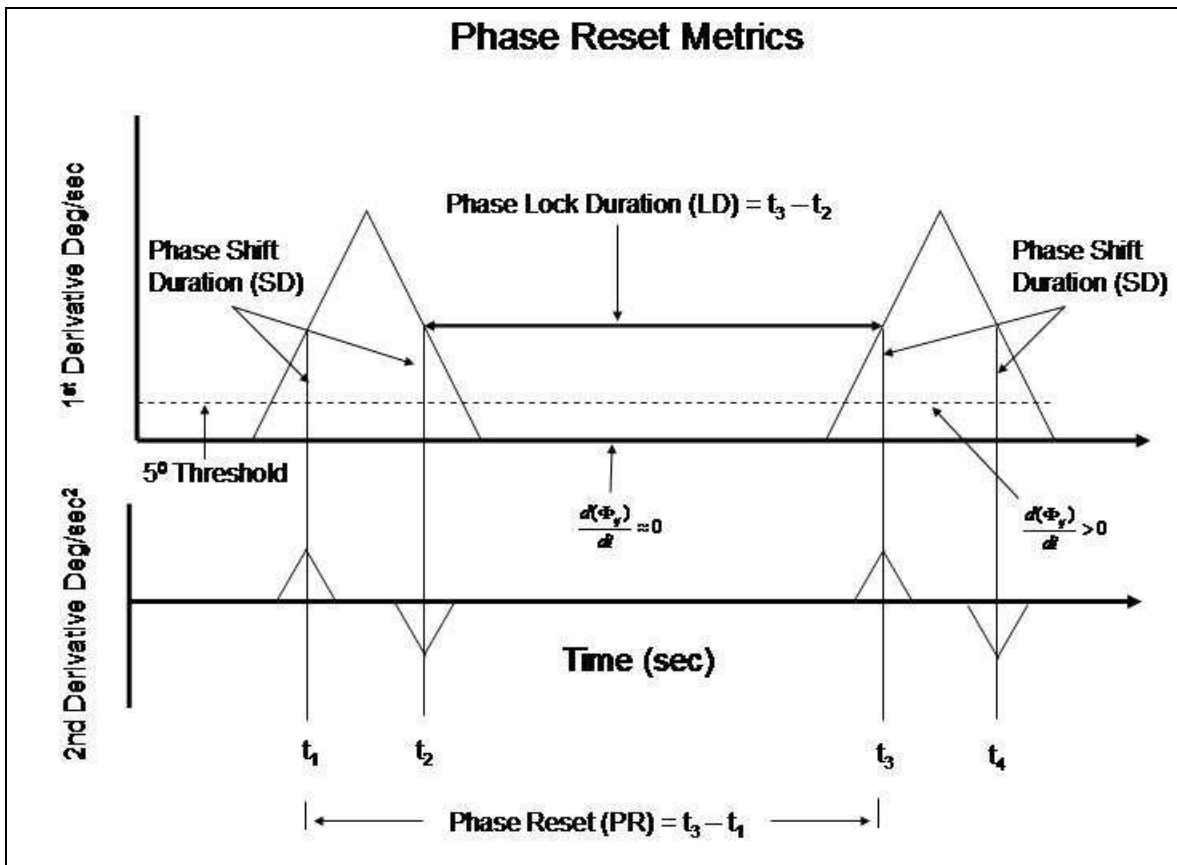
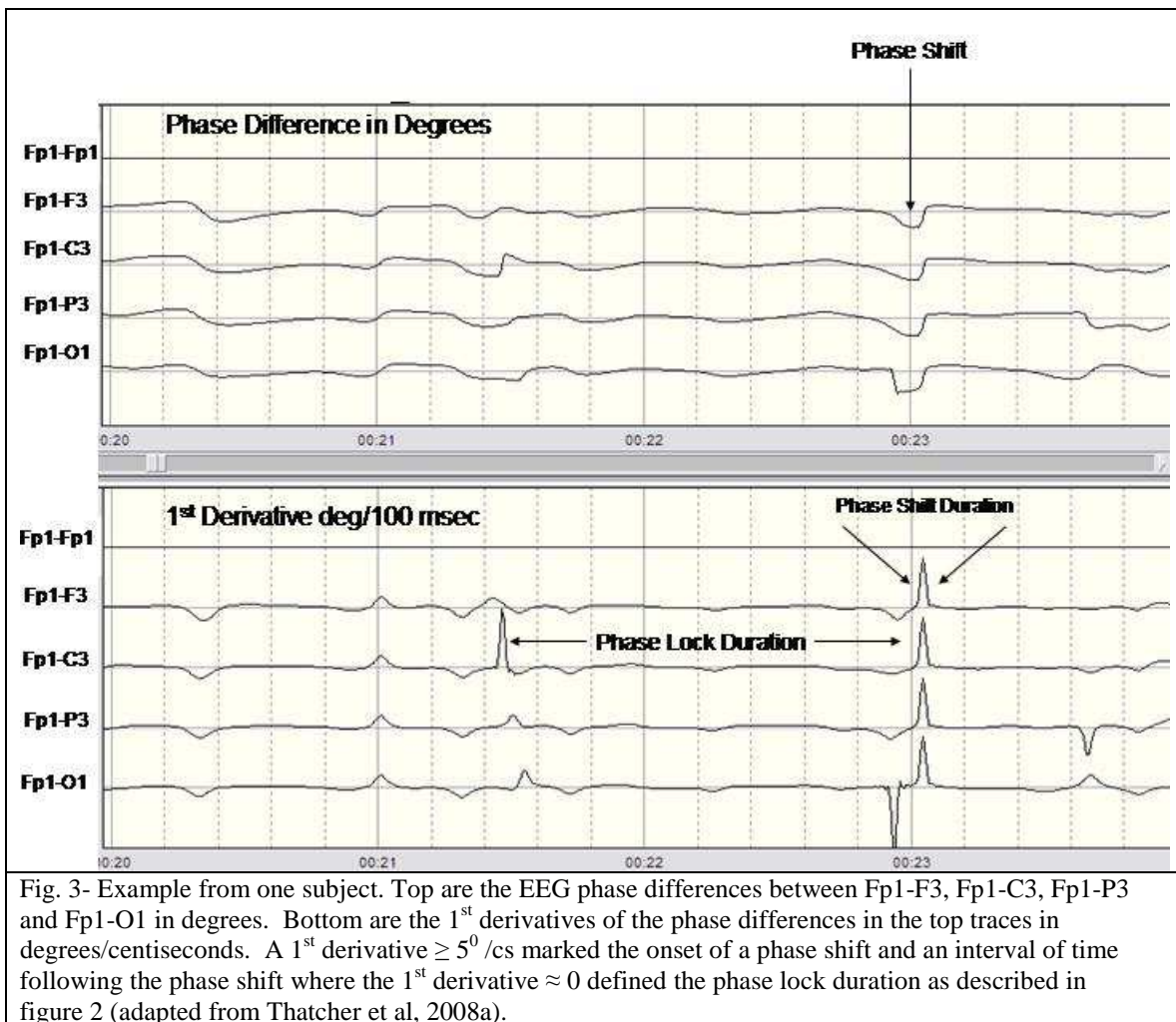


Fig. 2- Diagram of phase reset metrics. Phase shift (PS) onset was defined at the time point when a significant 1<sup>st</sup> derivative occurred ( $\geq 5^0$  /centisecond) followed by a peak in the 1<sup>st</sup> derivative, phase shift duration (SD) was defined as the time from onset of the phase shift defined by the positive peak of the 2<sup>nd</sup> derivative to the offset of the phase shift defined by the negative peak of the 2<sup>nd</sup> derivative. The phase lock duration (LD) was defined as the interval of time between the onset of a phase shift and the onset of a subsequent phase shift. Phase reset (PR) is composed of two events: 1- a phase shift and 2- a period of locking following the phase shift where the 1<sup>st</sup> derivative  $\approx 0$  or  $PR = SD + LD$ . Phase locking is defined when the absolute 1<sup>st</sup> derivative of the phase difference between two oscillators approximates zero  $|\frac{d(\Phi_{ij})}{dt}| \approx 0$ . Phase shift onset is defined when the absolute 1<sup>st</sup> derivative of the phase difference

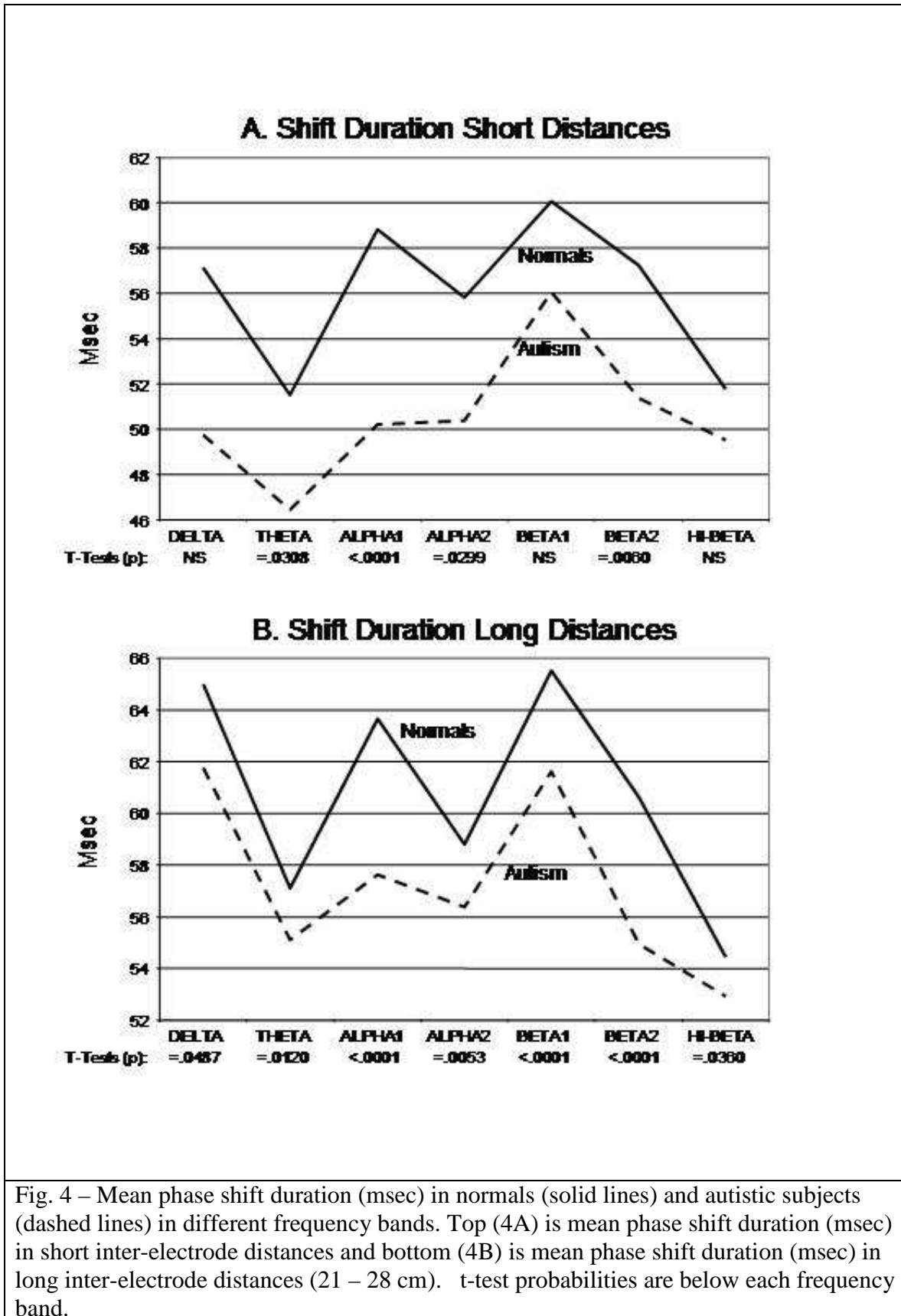
between two oscillators is greater than zero  $\frac{|d(\Phi_{ij})|}{dt} > 0$  (adapted from Thatcher et al, 2008a).



### 3.0 – Results

#### 3.1 – Autism vs Normal Phase Shift Duration

Figure 4A shows the mean phase shift duration in the various frequency bands for normals and autistic subjects for short inter-electrode distances (6 cm). Figure 4B shows the same measures but for long distance inter-electrode distances (18 cm to 24 cm). It can be seen that phase shift duration was consistently shorter in autistic subjects than in the normal subjects with the maximum difference being the alpha-1 frequency band (8 – 10 Hz) at both short and long inter-electrode distances. Multivariate analyses of variance showed an overall significant differences between normal subjects and autistic subjects ( $F = 2889.5$ ;  $P < .0001$ ) with a significant frequency main affect ( $F = 811.54$ ;  $P < .0001$ ) and a statistically significant inter-electrode distance main affect ( $F = 3,211.9$ ;  $P < .0001$ ) but no statistically significant hemispheric affect ( $F = 1.499$ ; NS).



### 3.2 – Autism vs Normal Phase Lock Duration

Figure 5A (top) shows the mean phase lock duration in the various frequency bands for normals and autistic subjects for short inter-electrode distances (6 cm). Figure 5B (bottom) shows the same measures but for long distance inter-electrode distances (18 cm to 24 cm). It can be seen that phase lock duration was consistently longer in autistic subjects than in the normal subjects with the maximum difference being the alpha-2 frequency band (10 - 12 Hz) at both short and long inter-electrode distances. Multivariate analyses of variance showed an overall significant differences between normal subjects and autistic subjects ( $F = 1,314.3$ ;  $P < .0001$ ) with a significant frequency main affect ( $F = 2,581.7$ ;  $P < .0001$ ) and a statistically significant inter-electrode distance main affect ( $F = 1,844.2$ ;  $P < .0001$ ) but no statistically significant hemispheric affect ( $F = 0.798$ ; NS). In contrast to phase shift duration (see figure 4), the largest differences between normal subjects and autistic subjects is in the alpha-2 frequency band (10 – 12 Hz) and not in the alpha-1 frequency band (8 – 10 Hz).

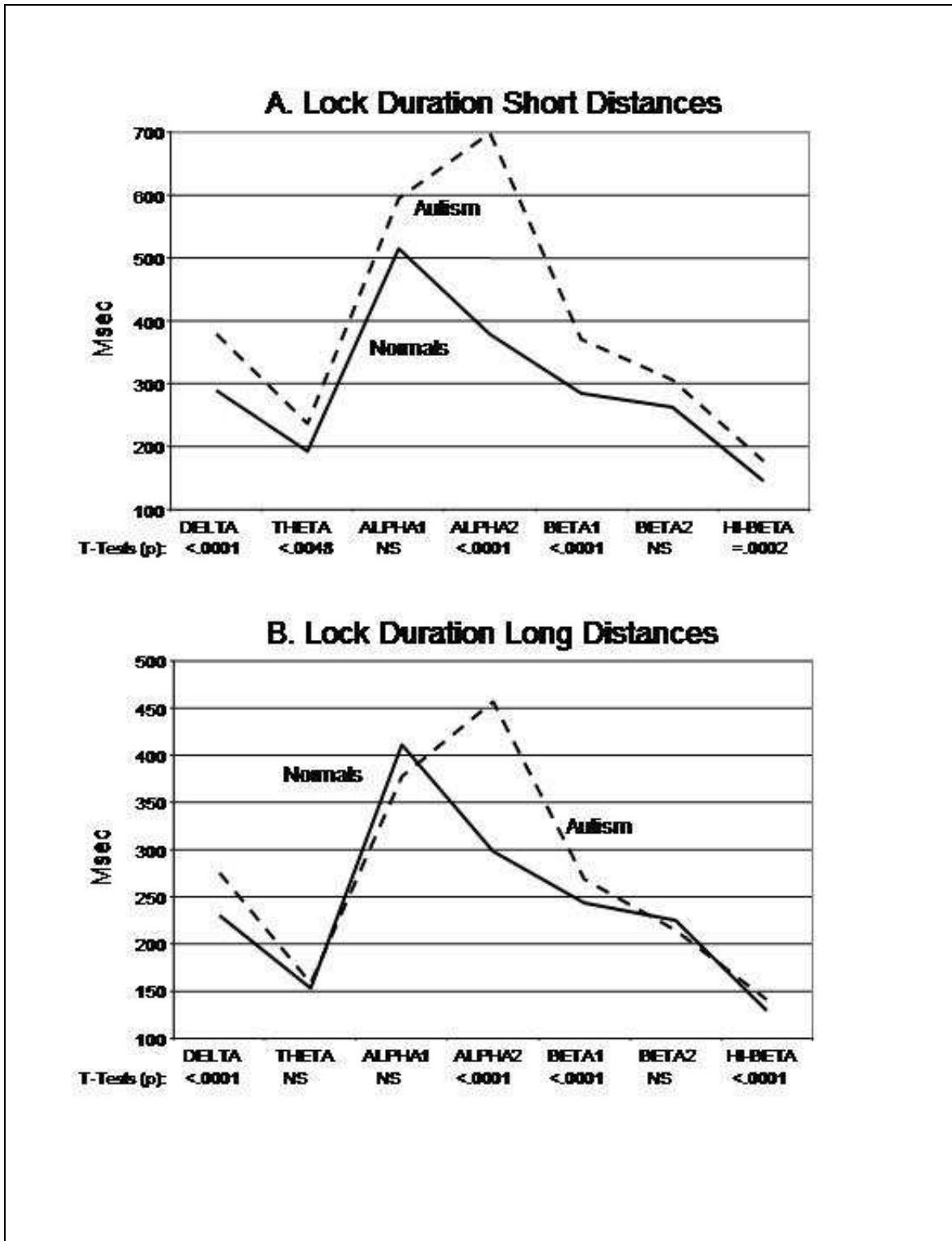


Fig. 5 – Mean phase lock duration (msec) in normals (solid lines) and autistic subjects (dashed lines) in different frequency bands. 5A is mean phase lock duration (msec) in short distance inter-electrode distances and 5B is mean phase lock duration (msec) in long inter-electrode distances (21 – 28 cm). t-test probabilities are below each frequency band.

**3.3 – Alpha-1 vs Alpha-2 Frequency bands and Phase Shift and Phase Lock Durations**

Figure 6A & B (left column) are histograms of phase shift duration in short and long inter-electrode distances in the alpha-1 frequency band (8 – 10 Hz). Figure 6C & D (right column) are histograms of phase lock duration in short and long inter-electrode distances in the alpha-2 frequency band (10 - 12 Hz). This figure shows that phase shift duration is shorter in autistic subjects than normal subjects in the alpha-1 frequency band (8 – 10 Hz) and that phase lock duration is longer in autistic subjects in the alpha-2 frequency band (10 – 12 Hz) independent of inter-electrode distance.

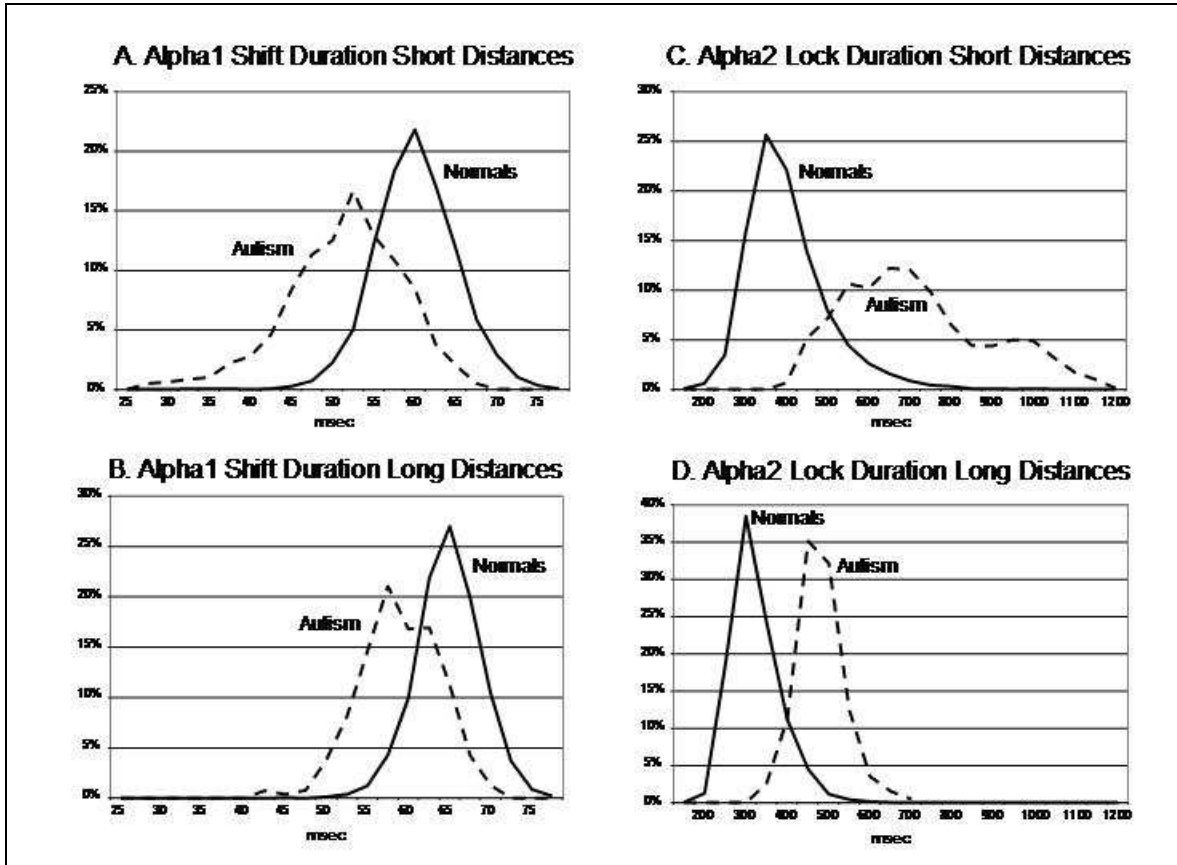


Fig. 6 - Histograms of the percentage of phase shift and phase lock duration measures in normal control and autistic subjects. The y-axis is the percentage of measures and the x-axis is phase shift duration (msec) in the alpha-1 (8-10 Hz) frequency band in A and B and phase lock duration (msec) in the alpha-2 (10-12 Hz) frequency band on the right in C and D. Top row (A & C) are histograms for short distance inter-electrode distances (6 cm) and the bottom row (B & D) are histograms for long inter-electrode distances (21-24 cm) in normals (solid lines) and autistic subjects (dashed lines).

**3.4 – Multi-Modal Distribution in Short Distance Lock Duration in Autistic Subjects**

The distribution of alpha-2 lock duration in the short distance (Fig. 6C) shows a bi-modal or tri-modal shape which indicates the presence of sub-populations in the autistic subjects. We sorted the magnitude of phase lock duration values in autistic subjects in order to evaluate the

multi-modal distribution and identified sub-populations that were present as a function of scalp location. Figure 7 shows the breakdown of the histograms of sub-populations of phase lock duration in short inter-electrode that were present in Figure 6C. This analysis identified three different sub-populations of phase lock duration: 1- a long phase locking sub-population in occipital-parietal pairings (O1/2-P3/4) with a peak mode of 1,000 msec; 2- an intermediate phase lock duration in short distance frontal regions (Fp1/2-F3/4) with a peak mode phase lock duration of 700 msec and 3- a shorter phase lock duration sub-population in the central regions (C3/4-F3/4) with a peak mode phase lock duration of 550 msec. This analysis demonstrates a significant anatomical difference in autistic subjects where the occipital-parietal distribution exhibits the

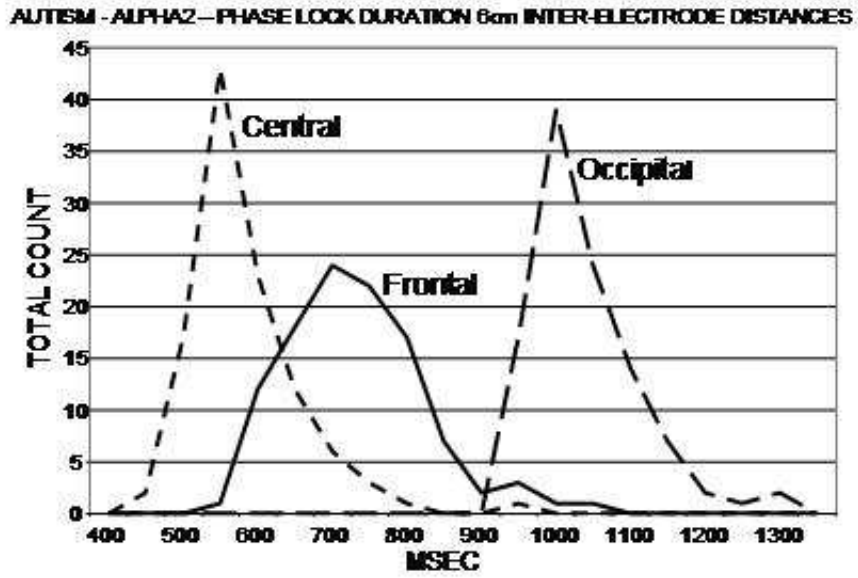


Fig. 7 - Histograms of the total number of phase lock duration (msec) values in short inter-electrode pairs (6 cm) from Occipital (O1/2-P3/4); Frontal (Fp1/2-F3/4) and Central (C3/4-F3/4) locations in the alpha-2 frequency band in autistic subjects.

Longest phase lock durations. T-tests between all pairings of three modes were statistically significant for all combinations ( $P < .001$ ).

#### **4.0 – Discussion**

The three primary findings of this study are: 1- there was shorter phase shift durations in autistic subjects vs. normals in all frequencies but especially in the alpha-1 frequency band (8 – 10 Hz); 2- there was longer phase lock durations in autistic patients vs normals only in the alpha-2 frequency band (10 - 12 Hz) and; 3- differences between autistic vs normal were present in local and distant inter-electrode pairs. No significant hemispheric effects were found between autistic and normal subjects.

#### **4.1 – Thalamic Synchronization and EEG Phase Reset**

As mentioned in the introduction, the development of EEG phase shift durations from birth to age 16 shows that there is only a 5 millisecond to 15 millisecond difference between short (6 cm) and long (24 cm) inter-electrode distances (Thatcher et al, 2008a; 2008b). Such short time differences (5 msec) at long inter-electrode distances (18 cm differences) can not be explained by a cortico-cortical connection system because conduction velocities greater than 1,000 meters/second are required. However, the thalamus is located in the center of the brain and coordinates all EEG rhythms and is only approximately 2 cm in the anterior-posterior plane with conduction velocities less than 1 meter/second that can explain the differences in phase shift duration measured at the scalp surface. Therefore, the thalamus is a prime if not the only candidate as the region of the brain responsible for EEG phase shift duration in which bursts of inhibitory neural activity results in shifts in frequencies of thalamo-cortical circuits and thus changes in EEG phase shift duration (Buzsaki, 2006; Thatcher et al, 2008b).

As mentioned in the introduction, phase shift and phase lock are basic synchronization mechanism that have been correlated in various frequency bands during cognitive tasks (Kahana, 2006; Kirschfeld, 2005; Tesche and Karhu, 2000), working memory (John, 1968; Rizzuto et al, 2003; Damasio, 1989; Tallon-Baudry et al, 2001), sensory-motor interactions (Vaadia et al, 1995; Roelfsema et al, 1997), hippocampal long-term potentiation (McCartney et al, 2004), brain development (Thatcher et al, 2008), consciousness (Cosmelli et al, 2004; Varela et al, 2001; John, 2002; 2005) and intelligence (Thatcher et al, 2008b). Thatcher et al (2008b) reported opposite relations between phase shift duration and phase lock duration and intelligence in normal subjects with a positive correlation between intelligence and phase shift duration and a negative correlation to phase lock duration. A neural synchronization model was developed in which it was hypothesized that long phase shift durations represent an expanded neural recruitment process in which larger populations of neurons are recruited the longer the phase shift duration. Phase shift duration was modeled by the duration of inhibitory burst activity in thalamo-cortical circuits in which the longer the inhibitory burst then the greater the phase shift duration (Thatcher et al, 2008b). Phase lock duration is mediated by cortical excitatory dendritic loops and represents periods of synchrony of selected clusters of neurons that temporarily mediate local and global functions. Too long of a phase lock period then there is less cognitive flexibility, less neural resource available to be allocated and reduced intelligence (Thatcher et al, 2008b). The present findings are consistent with the earlier studies from this laboratory (Thatcher et al, 2008a; 2008b) and indicate a deficiency of thalamo-cortical synchronization in autistic subjects in which there is a low degree of neural resource recruitment resulting in a reduced number of neurons that are synchronized at each moment of time coupled with a prolonged period of phase locking that results in reduced flexibility and reduced capacity to recruit available neural resources to be phase locked at each moment of time.

This same model can be applied to autistic subjects for particular brain regions and particular connections in which there are islands of normal phase shift and phase lock surrounded by a sea of deviant phase lock and phase shift durations. For example, individualized analysis of phase shift and phase lock durations in autistic subjects shows considerable spatial heterogeneity in the degree of deviation from normal which is consistent with the “idiot savant” type of behavior often observed in autistic subjects.

#### **4.2 – Unified Theory of Thalamo-Cortical Synchronization and Autism**

Buszaki (2006) and others (Kuffler and Edwards, 1958; Steriade, 2005) have shown a causal linkage between the duration of GABA mediated inhibitory postsynaptic potentials and the frequency of the EEG. GABA-B receptors involve potassium and calcium channels and produce IPSPs on the order of 50 msec to 200 msec with correlations to EEG frequencies in the theta to low beta frequency range (5 Hz to 20 Hz) (Bowery, 2002; Buszaki, 2006). The hi-beta (25 – 40 Hz) and Gamma (40 to 100 Hz) EEG frequencies have been correlated with GABA-A receptors that involve chlorine ionic channels and produce IPSPs on the order of 10 msec to 40 msec (Buszaki, 2006; Steriade, 2005; Mainen and Sejnowski, 1995; 1996; Thomson, 2000a; 2000b). Global or extrasynaptic thalamic GABA-A can produced hyperpolarization for sustained periods of time and infra-slow oscillations linked to sleep and drowsiness (Bright and Brickley, 2008). Deviations from the normal power spectrum in ASD subjects is consistent with the hypothesis of deficient GABA neurotransmitters as a unifying disorder in autistic subjects (DeLong, 2007; Kana et al, 2007; Orekhova et al, 2008). Although GABA deficiencies can be present in many brain regions and involve a variety of organ systems the present study only measured the cortical pyramidal cell electrical activity as modulated and synchronized by thalamo-cortical circuits (Steriade, 2005). Therefore, the results of the present study are consistent with a GABA receptor deficiency hypothesis in thalamo-cortical circuits that result in shortened phase shift durations in the thalamus and in lengthened phase lock durations in cortico-cortical and cortico-thalamic circuits in autistic subjects. The thalamus is a switching and coordinating system that can be visualized like the traffic control tower at a large airport or as “Grand Central Station” where trains arrive from distant locations and are delayed and timed to travel to different destinations. In the case of autistic subjects the trains arrive in grand central station but the train doors open only briefly before the train leaves the station. This results in a general reduction in information flow and disordered synchrony in widespread cortical regions. Lengthened phase locking is due to excessive iteration in cortical loops because more time is required to process information due to limited resources at each moment of time. This results in reduced efficiency and reduced speed of information processing, especially in the local networks of the occipital-parietal lobes as well as in global integration.

#### **4.3- Low Alpha Frequencies for Neural Resource Recruitment and High Alpha Frequencies for Resource Allocation**

Murias et al (2007) reported that the strongest EEG coherence differences were in the alpha-1 frequency band (8-10 Hz) between autistic and normal subjects. In the present study Alpha-1 (8 – 10 Hz) was the frequency band that showed the strongest differences in phase shift duration between the normal and autistic subjects (fig. 4). In contrast, the alpha-2 frequency band (10 – 12 Hz) showed the strongest differences in phase lock duration between normal control and autistic subjects (fig. 5). This indicates that the alpha-1 frequency band is more involved in the process of resource recruitment by rapid phase shifting while the alpha-2 frequency band involves resource allocation and binding by phase locking. Both processes are

deviant from normal in the autistic subjects and they appear to involve different brain networks with alpha-1 and phase shift durations being located primarily in the thalamus and alpha-2 and phase locking involving longer distant cortico-cortical and cortico-thalamic circuits.

#### **4.4 – Local vs Distant Information Processing in Autistic Subjects**

The multivariate analyses of variance demonstrated statistically significant differences between short vs long inter-electrode distances, especially in phase lock duration. In general higher statistical significance was present in short (6 cm) inter-electrode phase reset than in long inter-electrode distances (24 cm). Multi-modal distributions were present in short inter-electrode distances with the occipital-parietal regions exhibiting approximately three times greater phase lock duration than in normal control subjects (see Fig. 7). This finding indicates that autistic subjects recruit less neural resource at each moment of time and phase lock this reduce resource for long periods of time especially in local neural circuits in the occipital-parietal lobes. This may reflect a compensatory process in which reduced resources are phase locked for longer periods in order to process information and that therefore there is an inverse relationship between phase shift duration and phase lock duration. The finding of short phase shift duration and lengthened phase lock duration that is maximal in occipital-parietal regions is consistent with the behavioral characteristic of repetitive behaviors and excessive attention to detail and language problems. The reduced information processing capacity in the frontal lobes and in long distance networks is consistent with reduced social and global integration (Rapin and Dunn, 2003; Belmonte et al., 2004; Hill, 2004).

#### **4.5- Brain-Behavior Links to Autism**

As mentioned in the introduction, the symptoms of Autism are characterized by repetitive behavior, excessive focus on details and reduced social and global integration including deficits in executive function, language and social interactions (Rapin and Dunn, 2003; Belmonte et al., 2004; Hill, 2004). The dysfunctions of thalamo-cortical circuits in the brain can be linked to the core behavioral features of autism by the unifying theory of deficient GABAergic inhibition because the intensity and duration of inhibitory burst activity is what determines EEG frequency distributions, recruitment of neurons and EEG phase reset (Buzsaki, 2006; Steriade, 2005; Thatcher et al, 2008a; 2008b). For example, thalamic synchronization operates for both local and long distant connections and deficiencies in GABA can affect both local and global integration. Bursts of inhibition in thalamo-cortical circuits results in shifts in EEG frequencies and, therefore, deficient GABA can result in reduced phase shift duration and thus reduced recruitment of neural resources at each moment of time and in each perceptual frame. Finally, lengthened phase lock duration especially in local neural networks is a consequence of reduced phase shifting that underlay excessive attention to detail and reduced flexibility. Repetitive behaviors arise as a consequence of less recruitment of neural resources, thus giving rise to the need to repeat behaviors in order to learn and to store memories. All three of the major findings of this study: 1- reduced long distant connectivity, 2- reduced phase shift durations and 3 - lengthened phase locking especially in local connections can be explained by deficient GABAergic inhibition and when taken individually or in combination are consistent with the three characteristic symptoms of autism, namely, reduced global integration, excessive focus on detail and repetitive behaviors. Deficits in language and executive functions are likely due to the fact that the greatest deviations from normal phase locking and phase shift are in parietal-occipital regions for language and the frontal lobes involved in executive functioning. As

mentioned previously, analyses of individual autistic subjects shows a heterogeneity and a unique pattern of phase shift and phase lock so that “idiot savant” type behaviors are likely linked to the spatial distribution of islands of normal and abnormal information processing.

## 5.0 – References

Belmonte MK, Allen G, Beckel-Mitchener A, Boulanger LM, Carper RA, Webb SJ. (2004). Autism and abnormal development of brain connectivity. *J Neurosci.* 24(42):9228–31.

Bendat, J. S. & Piersol, A. G. (1980). *Engineering applications of correlation and spectral analysis*. New York: John Wiley & Sons.

Bloomfield, P. (2000). *Fourier Analysis of Time Series: An Introduction*, John Wiley & Sons, New York.

Bowery NG. (2002). "International Union of Pharmacology. XXXIII. Mammalian  $\gamma$ -Aminobutyric AcidB Receptors: Structure and Function". *Pharmacol Rev* 54 (2): 247–264.

Breakspear, M. and Terry, J.R. (2002a). Detection and description of non-linear interdependence in normal multichannel human EEG data. *Clin. Neurophysiol.*, 113(5): 735-753.

Breakspear, M. and Terry, J.R. (2002b). Nonlinear interdependence in neural systems: motivation, theory and relevance. *Int. J. Neurosci.*, 112(10): 1263-1284.

Breakspear, M. and Williams, L.M. (2004). A novel method for the topographic analysis of neural activity reveals formation and dissolution of ‘dynamic cell assemblies’. *J. Computational Neurosci.*, 16, 49-68.

Bright, D.P., M. Isabel Aller, M. and Brickley, S.G. (2007). Synaptic Release Generates a Tonic GABA<sub>A</sub> Receptor-Mediated Conductance That Modulates Burst Precision in Thalamic Relay Neurons. *The Journal of Neuroscience*, 27(10):2560 –2569.

Bright, D.P. and Brickley, S.G. (2008). Acting locally but sensing globally: impact of GABAergic synaptic plasticity on phasic and tonic inhibition in the thalamus. *J. Physiology*, 586(21): 5091-5099.

Brock J, Brown CC, Boucher J, and Rippon G. (2002). The temporal binding deficit hypothesis of autism. *Dev. Psychopathology*, 14(2): 209-224.

Brown C, Gruber T, Boucher J, Rippon G, Brock J. (2005). Gamma abnormalities during perception of illusory figures in autism. *Cortex*, 41(3): 364-376.

Buzsaki, G. (2006). *Rhythms of the Brain*, Oxford Univ. Press, New York.

Cantor, D.S., Thatcher, R.W. and Kaye, H. (1987). Computerized EEG Analyses of Autistic Children. *Int. J. Autism*, 114: 21-36.

Chavez, M., Le Van Quyen, M., Navarro, V., Baulac, M. and Martinerie, J. (2003). Spatio-temporal dynamics prior to neocortical seizures: amplitude versus phase couplings. *IEEE Trans. Biomed. Eng.* 50(5): 571-583.

Cosmelli, D., David, O., Lachaux, J.P., Martinerie, J., Garnero, L., Renault, B. and Varela, F. (2004). Waves of consciousness: ongoing cortical patterns during binocular rivalry. *Neuroimage*, 23(1): 128-140.

Damasio, A.R. (1989). Time-locked multiregional retroactivation: A systems-level proposal for the neural substrates of recall and recognition. *Cognition*, 33: 25-62.

DeLong, R. (2007). GABA(A) receptor alpha5 subunit as a candidate gene for autism and bipolar disorder: a proposed endophenotype with parent-of-origin and gain-of-function features, with or without oculocutaneous albinism. *Autism*, 11(2): 135-147.

Essl, M. and Rappelsberger, P. (1998). EEG coherence and reference signals: experimental results and mathematical explanations. *Med. Biol. Eng. Comput.*, 36: 399-406.

Freeman, W.J. (2003). Evidence from human scalp electroencephalograms of global chaotic itinerancy. *Chaos*, 13(3): 1067- 1077.

Freeman W.J. and Rogers, L.J. (2002). Fine temporal resolution of analytic phase reveals episodic synchronization by state transitions in gamma EEGs. *J. Neurophysiol*, 87(2): 937-945.

Freeman, W.J., Burke, B.C. and Homes, M.D. (2003). Aperiodic phase re-setting in scalp EEG of beta-gamma oscillations by state transitions at alpha-theta rates. *Hum Brain Mapp.* 19(4):248-272.

Freeman, W.J., Homes, M.D., West, G.A. and Vanhatlo, S. (2006). Fine spatiotemporal structure of phase in human intracranial EEG. *Clin Neurophysiol.* 117(6):1228-1243.

Golomb, D., Ahissar, E. and Kleinfeld, D. (2006) Coding of stimulus frequency by latency in thalamic networks through the interplay of GABAB-mediated feedback and stimulus shape. *J. Neurophysiol.*, 95(3): 1735-1750.

Granger, C.W.J. and Hatanka, M. (1964). *Spectral Analysis of Economic Time Series*, Princeton University Press, New Jersey.

Gray, C., Konig, P., Engel, A.K. and Singer, W. (1989). Oscillatory responses in cat visual cortex exhibit inter-columnar synchronization which reflects global stimulus properties. *Nature (London)*, 223: 334-337.

Hardan AY, Minshew NJ, Melhem NM, Srihari S, Jo B, Bansal R, Keshavan MS, Stanley JA. (2008). An MRI and proton spectroscopy study of the thalamus in children with autism. *Psychiatry Res.*, 163(2): 97-105.

Hastings, J.A. and Simons, D.J. (1998). Thalamic Relay of Afferent Responses to 1- to 12-Hz Whisker Stimulation in the Rat. *J. Neurophysiol.*, 80(2): 1016-1019.

Hill EL. (2004). Executive dysfunction in autism. *Trends Cogn Sci.* 8(1):26–32.

Hughes, J.R. (2007). Autism: the first firm finding = underconnectivity? *Epilepsy Behav.*, 11(1): 20-24.

John, E.R. (1968), *Mechanisms of Memory.* Academic Press, New York.

John, E.R. (2002). The neurophysics of consciousness. *Brain Res Brain Res Rev.* 39(1):1-28.

John, E.R. (2005). From synchronous neural discharges to subjective awareness? *Progress in Brain Research*, Vol. 150: 143-171.

Just MA, Cherkassky VL, Keller TA, Kana RK, Minshew NJ. (2007). Functional and anatomical cortical underconnectivity in autism: evidence from an fMRI study of an executive function task and corpus callosum morphometry. *Cere. Cortex*, 17(4): 951-961.

Kahana, M.J. (2006). The cognitive correlates of human brain oscillations. *J. Neurosci.*, 26:1669-1672.

Kamiński, M. and Blinowska, K.J. (1991). A new method of the description of the information flow in the brain structures. *Biol.Cybern.* 65, 203-210.

Kirschfeld, K. (2005). The physical basis of alpha waves in the electroencephalogram and the origin of the "Berger effect"., *Biol. Cybern.*, 92(3):177-185.

Kana RK, Keller TA, Minshew NJ, Just MA. (2007). Inhibitory control in high-functioning autism: decreased activation and underconnectivity in inhibition networks. *Biol. Psychiatry*, 62(3): 198-203.

Kana RK, Keller TA, Cherkassky VL, Minshew NJ, Adam Just M. (2008). Atypical frontal-posterior synchronization of Theory of Mind regions in autism during mental state attribution. *Soc. Neurosci.*, 3: 1-8.

Kleinmans, NM, Schweinsburg BC, Cohen DN, Müller RA, Courchesne E. (2007). N-acetyl aspartate in autism spectrum disorders: regional effects and relationship to fMRI activation. *Brain Res.* 1162:85-97

Kuffler SW and Edwards C (1958). Mechanism of gamma-aminobutyric acid (GABA) action and its relation to synaptic inhibition. *J Neurophysiol* 21 (6): 589–610.

Leré C, El Bahh B, Le Gal La Salle G, Rougier A. (2002). A model of 'epileptic tolerance' for investigating neuroprotection, epileptic susceptibility and gene expression-related plastic changes. *Brain Res Brain Res Protoc.*, 9(1):49-56.

Le van Quyen, M. (2003). Disentangling the dynamic core: A research program for a neurodynamics at the large-scale. *Biol. Res.*, 36: 67-88.

Le Van Quyen, M., Foucher, J., Lachaux, J.-P., Rodriguez, E., Lutz, A., Martinerie, J. and Varela, F.J. (2001a). Comparison of Hilbert transform and wavelet methods for the analysis of neuronal synchrony. *J. Neurosci. Methods*, 111(2): 83-89.

Le Van Quyen, M., Martinerie, J., Navarro, V. and Varela, F.J. (2001b). Characterizing neurodynamic changes before seizures. *J. Clin. Neurophysiol.*, 18(3): 191-208.

Lopes Da Silva, F.H. and Pijn, J.P. (1995). *Handbook of Brain Theory and Neural Networks*. MIT Press, Arbib, Cambridge.

Lorente, P., Lacampagne, A., Pouzeratte, Y. Richards, S, Malitschek, B., Kuhn, R., Bettler, B. and Vassort, G. (2000). Gamma-aminobutyric acid type B receptors are expressed and functional in mammalian cardiomyocytes. *Proc. Natl. Acad. Sci, U.S.A.*, 97(15): 8664-8669.

Mainen, Z.F. and Sejnowski, T.J. (1995). Reliability of spike timing in neocortical neurons. *Science*, 268: 1503-1506.

Mainen, Z.F. and Sejnowski, T.J. (1996). Influence of dendritic structure on firing pattern in model neocortical neurons. *Nature*, 382: 363-366.

McCartney, H., Johnson, A.D., Weil, Z.M. and Givens, B. (2004). Theta reset produces optimal conditions for long-term potentiation. *Hippocampus*, 14(6):684-697.

Miller, R. (1996); Cortico-thalamic interplay and the security of operation of neural assemblies and temporal chains in the cerebral cortex. *Biol. Cybern.*, 75:263-275.

Minschew, N.J. and Pettegrew, J.W. (1995). Nuclear magnetic resonance spectroscopy studies of cortical development. In: Thatcher, R.W., Lyon, G.R., Rumsey, J. and Krasnegor, N. Editors. *Developmental Neuroimaging: Mapping the Development of Brain and Behavior*, Academic Press, Florida, pp. 107-126.

Minschew, N.J. and Williams, D.L. (2007). The new neurobiology of autism: cortex, connectivity and neuronal organization. *Arch. Neurol.*, 64(7): 945-950.

Murias M, Webb SJ, Greenson J, Dawson G. (2007). Resting state cortical connectivity reflected in EEG coherence in individuals with autism. *Biol. Psychiat.*, 62(3): 270-273.

Netoff, T.I. and Schiff, S.J. (2002). Decreased neuronal synchronization during experimental seizures. *J. Neurosci.*, 22(16): 7297-7307.

Ng GY, Bertrand S, Sullivan R, Ethier N, Wang J, Yergey J, Belley M, Trimble L, Bateman K, Alder L, Smith A, McKernan R, Metters K, O'Neill GP, Lacaille JC, Hébert TE. (2001). Gamma-aminobutyric acid type B receptors with specific heterodimer composition and postsynaptic actions in hippocampal neurons are targets of anticonvulsant gabapentin action. *Mol. Pharmacol.*, 59(1): 144-152.

Okada, M., Onodera, K., Van Renterghem C., Sieghart, W. and Takahashi, T. (2000). Functional correlation of GABA(A) receptor  $\alpha$  subunits expression with the properties of IPSCs in the developing thalamus. *J. Neurosci.*, 20:2202-2208.

Oppenheim, A.V. and Schaffer, R.W. (1975). *Digital Signal Processing*, Prentice-Hall, London.

Orekhova EV, Stroganova TA, Nygren G, Tsetlin MM, Posikera IN, Gillberg C, Elam M. (2007). Excess of high frequency electroencephalogram oscillations in boys with autism. *Biol. Psychiatry*, 62(9): 1022-1029.

Orekhova EV, Stroganova TA, Prokofyev AO, Nygren G, Gillberg C, Elam M. (2008). Sensory gating in young children with autism: relation to age, IQ and EEG gamma oscillations. *Neurosci Lett.*, 434(2): 218-223.

Otnes, R.K. and Enochson, L. (1978). *Applied Time Series Analysis*, John Wiley & Sons, New York.

Otsuka H, Harada M, Mori K, Hisaoka S, Nishitani H. (1999). Brain metabolites in the hippocampus-amygdala region and cerebellum in autism: an <sup>1</sup>H-MR spectroscopy study. *Neuroradiology*. 41(7):517-519.

Pikovsky, A., Rosenblum, M. and Kurths, J. (2003). *Synchronization: A universal concept in nonlinear sciences*. Cambridge Univ. Press, New York.

Press, W. H., Teukolsky, S. A., Vetterling, W. T. & Flannery, B. P. (1994). *Numerical recipes in C*. Cambridge, U.K., Cambridge University Press.

Perich-Alsina J, Aduna de Paz M, Valls A, Muñoz-Yunta JA. (2002). Thalamic spectroscopy using magnetic resonance in autism. *Rev. Neurol.*, 34, Suppl 1:S68-71

Rappelsberger, P. (1989). The reference problem and mapping of coherence: A simulation study. *Brain Topog.* 2(1/2): 63-72.

Rapin I, Dunn M. (2003). Update on the language disorders of individuals on the autistic spectrum. *Brain Dev.* 25:166-72.

Rippon G, Brock J, Brown C, Boucher J. (2007). Disordered connectivity in the autistic brain: challenges for the "new psychophysiology". *Int. J. Psychophysiol.*, 63(2): 164-172.

Rizzuto, D.S., Madsen, J.R., Bromfield, E.B., Schultz-Bonhage, A., Seelig, D., Aschenbrenner-Scheibe, R. and Kahana, M.J. (2003). Reset of human neocortical oscillations during a working memory task. *Proc Natl Acad Sci U S A.* 100(13):7931-7936.

Roelfsmema, P.R., Engel, A.K., Konig, P. and Singer, W. (1997). Visuomotor integration is associated with zero time-lag synchronization among cortical areas. *Nature*, 385(6612): 157-161.

Rudrauf, D., Douiri, A., Kovach, C., Lachaux, J.P., Cosmelli, D., Chavez, A., Renault, B., Martinerie, J. and Le Van Quyen, M. (2006). Frequency flows and the time-frequency dynamics of multivariate phase synchronization in brain signals. *Neuroimage*, 31: 209-227.

Savitzky, A. and Golay, M.J.E. (1964). Smoothing and differentiation of data by simplified least squares procedures, *Analytic Chemistry*, 36: 1627-1639.

Stam CJ, van der Made Y, Pijnenburg YAL, Scheltens Ph. (2002a). EEG synchronization in mild cognitive impairment and Alzheimer's disease. *Acta Neurol. Scand.* 106: 1-7.

Stam CJ, van Cappellen vanWalsumAM, Pijnenburg YAL, Berendse, HW, de Munck JC, Scheltens Ph, van Dijk BW (2002b). Generalized synchronization of MEG recordings in Alzheimer's disease: Evidence for involvement of the gamma band. *J. Clin. Neurophysiol* 19: 562-574.

Stam, C.J. and de Bruin, E.A. (2004). Scale-free dynamics of global functional connectivity in the human brain. *Hum. Brain Map.* 22:97-109.

Steriade, M., Gloor, P., Linas, R., Lopes da Silva, F.H. and Mesulam, M.M. (1990). Basic mechanisms of cerebral rhythmic activity. *EEG and Clin. Neurophysiol.*, 76: 481-508.

Steriade, M. (2005). Cellular substrates of brain rhythms. In: *Electroencephalography: Basic principles, clinical applications and related fields.* E. Niedermeyer and F. Lopes Da Silva (Eds.), Lippincott Williams & Wilkins, New York, pp. 31-83.

Tallon-Baudry, C., Bertrand, O., and Fischer, C. (2001). Oscillatory synchrony between human extrastriate areas during visual short-term memory maintenance. *J. Neurosci.*, 21(20): RC177.

Tass, P.A. (1997). *Phase Resetting in Medicine and Biology*, Springer-Verlag, Berlin.

Tass, P.A., Rosenblum, M.G., Weule, J., Kurths, J., Pikovsky, A., Volkmann, J., aSchnitzler, A. and Freund, H.J. (1998). Detection of n:m phase locking from noisy data: application to magnetoencephalography. *Phys. Rev. Lett.*, 81(15): 3291-3294.

Tesche, C.D. and Karhu, J. (2000). Theta oscillations index human hippocampal activation during a working memory task. *Proc Natl Acad Sci U S A.* 18;97(2):919-924.

Thatcher, R.W., Walker, R.A. and Guidice, S. (1987). Human cerebral hemispheres develop at different rates and ages. *Science*, 236: 1110-1113.

Thatcher, R.W., Walker, R.A., Biver, C., North, D., Curtin, R., (2003). Quantitative EEG Normative databases: Validation and Clinical Correlation, *J. Neurotherapy*, 7 (No. ¾): 87 – 122.

Thatcher, R.W., North, D. and Biver, C. J., (2007). Development of cortical connections as measured by EEG coherence and phase. *Human Brain Mapping*, Oct., early publication.

Thatcher, R.W., North, D., and Biver, C. (2008a). Self organized criticality and the development of EEG phase reset. *Human Brain Mapp.*, Jan 24, 2008.

Thatcher, R.W., North, D., and Biver, C. (2008b). Intelligence and EEG phase reset: A two-compartmental model of phase shift and lock, *NeuroImage*, 42(4): 1639-1653.

Thomson, A.M. (2000a). Facilitation, augmentation and potentiation at central synapses. *Trends Neurosci.*, 23: 305-312.

Thomson, A.M. (2000b). Molecular frequency filters at central synapses. *Prog. Neurobiol.*, 62: 159-196.

Vaadia, E., Haalman, L., Abeles, M., Bergman, H., Prut, Y., Slovin, H. and Aertsen, A. (1995). Dynamics of neuronal interactions in monkey cortex in relation to behavior events. *Nature*, 373(6514): 515-518.

Vandenbroucke MW, Scholte HS, van Engeland H, Lamme VA, Kemner C. (2008). A neural substrate for atypical low-level visual processing in autism spectrum disorder. *Brain*, 131(Pt 4):1013-1024.

Varela, F.J. (1995). Resonant cell assemblies: a new approach to cognitive functions and neuronal synchrony. *Biol. Res.*, 28(1): 81-95.

Varela, F.J., Lachaux, J.-P., Rodriguez, E., and Martinerie, J. (2001). The brainweb: phase synchronization and large-scale integration. *Nat. Rev., Neurosci.*, 2(4): 229-239.

Welsh, J.P., Ahn, E.S. and Placantonakis, D.G. (2005). Is autism due to brain desynchronization. *Int. J. Dev. Neurosci.*, 23(2-3): 253-263

## 6.0 – Figure Legends

**Figure One:** – Illustrations of phase reset. Left is the unit circle in which there is a clustering of phase angles and thus high coherence as measured by the length of the unit vector  $r$ . The top row is an example of phase reduction and the top right is a time series of the approximated 1<sup>st</sup> derivative of the instantaneous phase differences for the time series  $t_1, t_2, t_3, t_4$  at mean phase angle =  $45^0$  and  $t_5, t_6, t_7, t_8$  at mean phase angle =  $10^0$ . The vector  $r_1 = 45^0$  occurs first in time and the vector  $r_2 = 10^0$  and  $135^0$  (see bottom left) occurs later in time. Phase reset is defined by a sudden change in phase difference followed by a period of phase locking. The onset of Phase Reset is between time point 4 and 5 where the 1<sup>st</sup> derivative is a maximum. The 1<sup>st</sup> derivative near zero is when there is phase locking and little change in phase difference over time. The bottom row is an example of phase advancement and the bottom right is the 1<sup>st</sup> derivative time series. The sign or direction of phase reset in a pair of EEG electrodes is arbitrary since there is no absolute “starting point” and phase shifts are often “spontaneous” and not driven by external events, i.e., self-organizing criticality. When the absolute 1<sup>st</sup> derivative  $\approx 0$  then two oscillating events are in phase locking and represent a stable state independent of the direction of phase shift (adapted from Thatcher et al, 2008a).

**Figure Two:** Diagram of phase reset metrics. Phase shift (PS) onset was defined at the time point when a significant 1<sup>st</sup> derivative occurred ( $\geq 5^0$  /centisecond) followed by a peak in the 1<sup>st</sup> derivative, phase shift duration (SD) was defined as the time from onset of the phase shift defined by the positive peak of the 2<sup>nd</sup> derivative to the offset of the phase shift defined by the negative peak of the 2<sup>nd</sup> derivative. The phase lock duration (LD) was defined as the interval of time between the onset of a phase shift and the onset of a subsequent phase shift. Phase reset (PR) is composed of two events: 1- a phase shift and 2- a period of locking following the phase shift where the 1<sup>st</sup> derivative  $\approx 0$  or  $PR = SD + LD$ . Phase locking is defined when the absolute 1<sup>st</sup> derivative of the phase difference between two oscillators approximates zero  $\frac{|d(\Phi_{ij})|}{dt} \approx 0$ .

Phase shift onset is defined when the absolute 1<sup>st</sup> derivative of the phase difference between two oscillators is greater than zero  $\frac{|d(\Phi_{ij})|}{dt} > 0$  (adapted from Thatcher et al, 2008a).

**Figure Three:** Example from one subject. Top are the EEG phase differences between Fp1-F3, Fp1-C3, Fp1-P3 and Fp1-O1 in degrees. Bottom are the 1<sup>st</sup> derivatives of the phase differences in the top traces in degrees/centiseconds. A 1<sup>st</sup> derivative  $\geq 5^0$  /cs marked the onset of a phase shift and an interval of time following the phase shift where the 1<sup>st</sup> derivative  $\approx 0$  defined the phase synchrony interval as described in figure 2 (adapted from Thatcher et al, 2008a).

**Figure Four:** Mean phase shift duration (msec) in normals (solid lines) and autistic subjects (dashed lines) in different frequency bands. Top is mean phase shift duration (msec) in short inter-electrode distances and bottom is mean phase shift duration (msec) in long inter-electrode distances (21 – 28 cm). t-test probabilities are below each frequency band.

**Figure Five:** Mean phase lock duration (msec) in normals (solid lines) and autistic subjects (dashed lines) in different frequency bands. Top is mean phase lock duration (msec) in short distance inter-electrode distances and bottom is mean phase lock duration (msec) in long inter-electrode distances (21 – 28 cm). t-test probabilities are below each frequency band.

**Figure Six:** Histograms of the percentage of phase shift and phase lock duration measures in normal control and autistic subjects. The y-axis is the percentage of measures and the x-axis is phase shift duration (msec) in the alpha-1 (8-10 Hz) frequency band in A and B and phase lock duration (msec) in the alpha-2 (10-12 Hz) frequency band on the right in C and D. Top row (A & C) are histograms for short distance inter-electrode distances (6 cm) and the bottom row (B & D) are histograms for long inter-electrode distances (21-24 cm) in normals (solid lines) and autistic subjects (dashed lines).

**Figure Seven:** Histograms of the total number of phase lock duration (msec) values in short inter-electrode pairs (6 cm) from O1/2-P3/4; Fp1/2-F3/4 and C3/4-F3/4 in the alpha-2 (10-12 Hz) frequency band in autistic subjects.